

Electronic Supplementary Material

Orientational self-sorting: formation of structurally defined Pd₄L₈ and Pd₆L₁₂ cages from low-symmetry dipyridyl ligands

Ru-Jin Li,^a Adam Marcus,^b Farzaneh Fadaei-Tirani,^a and Kay Severin*

^a *Institut of Chemical Sciences and Engineering, École Polytechnique Fédérale de Lausanne (EPFL), 1015 Lausanne, Switzerland*

^b *Institut of Mathematics, EPFL, 1015 Lausanne, Switzerland*

Table of Contents

1 General	2
2 Syntheses	3
2.1 Synthesis of the ligands.....	3
2.2 Syntheses of the cages	9
3 Titration	17
4 Control experiments	18
5 Analysis of potential isomers	20
4.1 Translation into vectors and matrices	20
4.2 Integer labels.....	21
4.3 Results	21
6 Crystallographic analyses	24
7 References	26

1 General

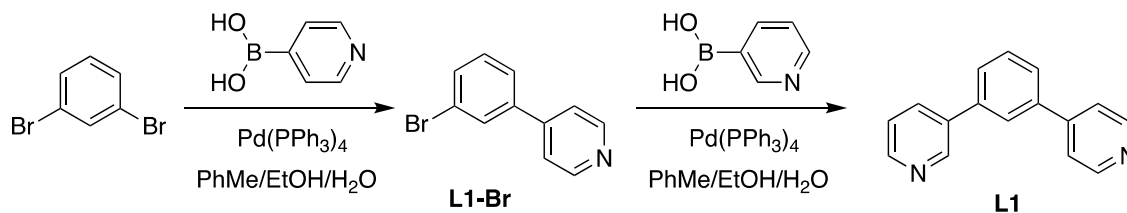
All chemicals were obtained from commercial sources and used without further purification unless stated otherwise.

NMR spectra were measured on a Bruker Avance III HD spectrometer (^1H : 400 MHz, ^{13}C : 101 MHz) equipped with a BBFO-Plus_z 5 mm probe, a Bruker Avance III spectrometer (^1H : 400 MHz) equipped with a BBFO_z 5 mm probe, a Bruker Avance III spectrometer (^1H : 400 MHz) equipped with a BBI_z 5 mm probe, and a Bruker Avance III spectrometer (^1H : 400 MHz) equipped with a Prodigy BBO 5 mm cryoprobe. The chemical shifts are reported in parts per million (ppm) using the solvent residual signal as a reference.

High resolution mass spectrometry experiments were carried out using a hybrid ion trap-Orbitrap Fourier transform mass spectrometer, Orbitrap Elite (Thermo Scientific) equipped with a TriVersa Nanomate (Advion) nano-electrospray ionization source. Mass spectra were acquired with a minimum resolution setting of 120,000 at 400 m/z . To reduce the degree of analyte gas phase reactions leading to side products unrelated to solution phase, the transfer capillary temperature was lowered to 50 °C. Experimental parameters were controlled via standard and advanced data acquisition software.

2 Syntheses

2.1 Synthesis of the ligands



L1-Br : 1,3-Dibromobenzene (472 mg, 2.00 mmol), pyridin-4-ylboronic acid (123 mg, 1.00 mmol), Pd(PPh₃)₄ (115 mg, 995 μmol), and K₂CO₃ (0.6 g, 4.3 mmol) were combined in a 50 mL Schlenk tube. After vacuum/backfilling with N₂ for three times, 20 mL degassed toluene/EtOH/H₂O (2:1:1) was added with a syringe. The mixture was heated at 85 °C overnight. The reaction was cooled to RT, quenched with water, extracted with DCM (2 x 50 mL), washed with water (2 x 50 mL) and brine (50 mL), and dried over MgSO₄. The solvent was removed under reduced pressure, and the residue was purified by column chromatography on silica to yield **L1-Br** as a white powder (318 mg, 1.36 mmol, 68%). ¹H NMR (400 MHz, CDCl₃) δ 8.74 (d, *J* = 5.6 Hz, 2H), 7.84 (t, *J* = 1.9 Hz, 1H), 7.77 (d, *J* = 5.5 Hz, 2H), 7.68 (d, *J* = 8.0 Hz, 1H), 7.62 (d, *J* = 7.8 Hz, 1H), 7.44 (t, *J* = 7.9 Hz, 1H). ¹³C NMR (101 MHz, CDCl₃) δ 145.87, 138.42, 133.74, 131.23, 130.57, 126.11, 123.90, 123.10. ESI-MS: *m/z* calculated for C₁₁H₉NBr [M+H]⁺ 233.99, found 233.99.

L1 : Pyridin-3-ylboronic acid (185 mg, 1.51 mmol), **L1-Br** (300 mg, 1.28 mmol), Pd(PPh₃)₄ (81 mg, 70 μmol), and K₂CO₃ (0.6 g, 4.3 mmol) were combined in a 50 mL Schlenk tube. After vacuum/backfilling with N₂ for three times, 20 mL degassed toluene/EtOH/H₂O (2:1:1) was added with a syringe. The mixture was heated at 85 °C overnight. The reaction was cooled to RT, quenched with water, extracted with DCM (2 x 50 mL), washed with water (2 x 50 mL) and brine (50 mL), and dried over MgSO₄. The solvent was removed under reduced pressure, and the residue was purified by column chromatography on silica to yield **L1** as a colorless oil (179 mg, 0.77 mmol, 60%). ¹H NMR (400 MHz, CDCl₃) δ 8.91 (dd, *J* = 2.4, 0.9 Hz, 1H), 8.74 – 8.69 (m, 2H), 8.65 (dd, *J* = 4.9, 1.6 Hz, 1H), 7.94 (ddd, *J* = 7.9, 2.4, 1.6 Hz, 1H), 7.83 (td, *J* = 1.8, 0.6 Hz, 1H), 7.72 – 7.62 (m, 3H), 7.62 – 7.58 (m, 2H), 7.42 (ddd, *J* = 7.9, 4.8, 0.9 Hz, 1H). ¹³C NMR (101 MHz, CDCl₃) δ 149.94, 148.97, 148.69, 148.37, 139.11, 139.07, 136.32, 134.77, 130.15, 128.18, 126.97, 126.10, 123.87, 122.05. ESI-MS: *m/z* calculated for C₁₆H₁₃N₂ [M+H]⁺ 233.11, found 233.11.

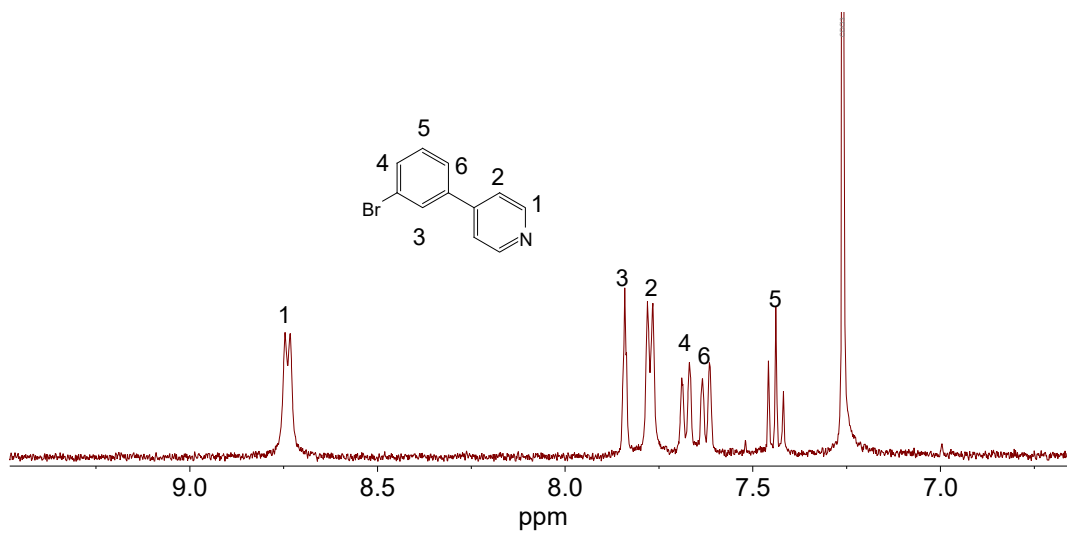


Figure S1. ¹H NMR (400 MHz, CDCl₃) spectrum of **L1-Br**.

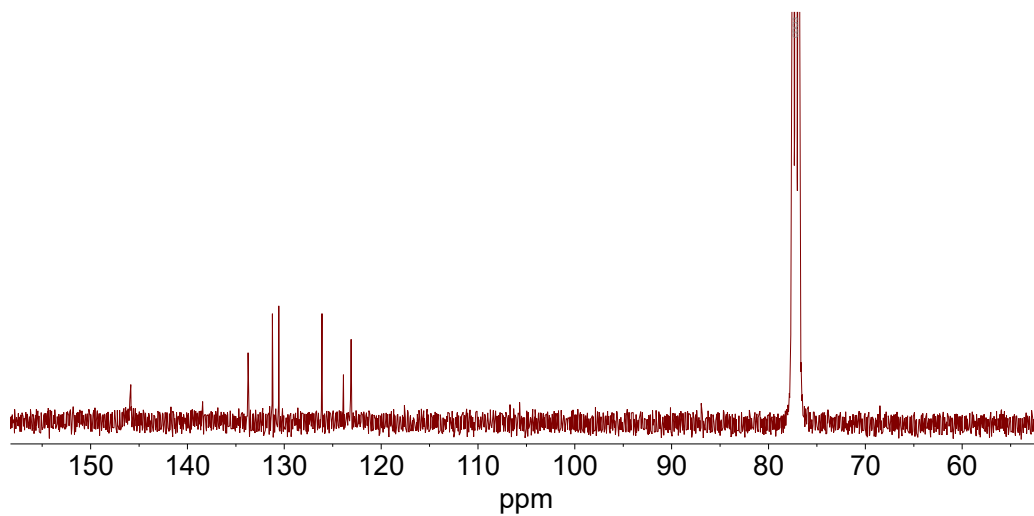


Figure S2. ¹³C NMR (101 MHz, CDCl₃) spectrum of **L1-Br**.

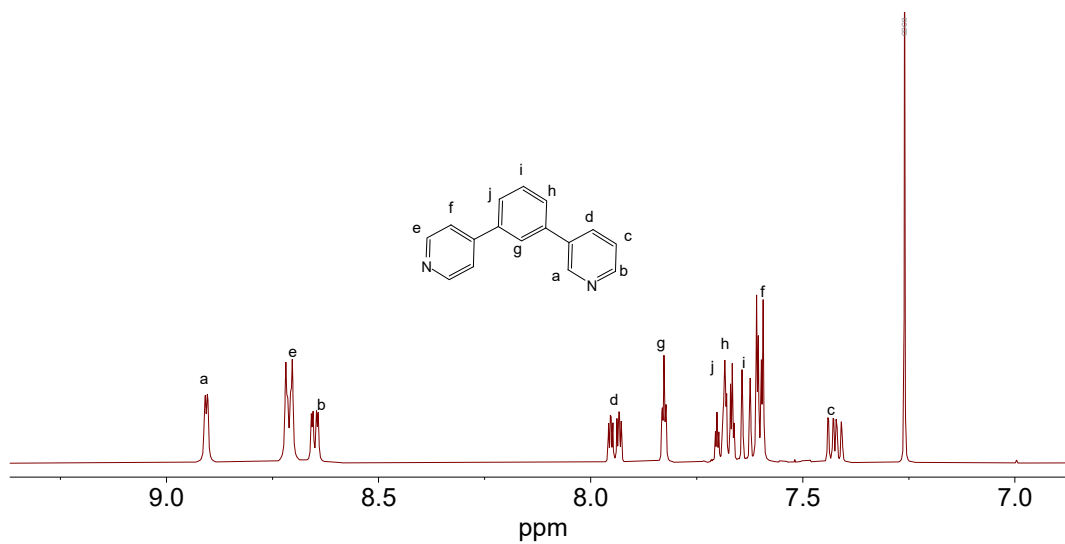


Figure S3. ¹H NMR (400 MHz, CDCl₃) spectrum of ligand L1.

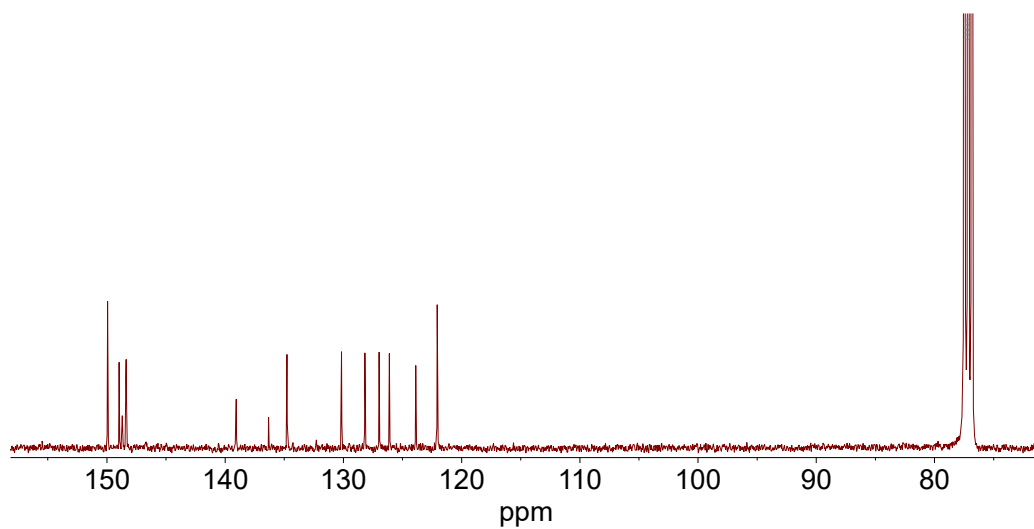
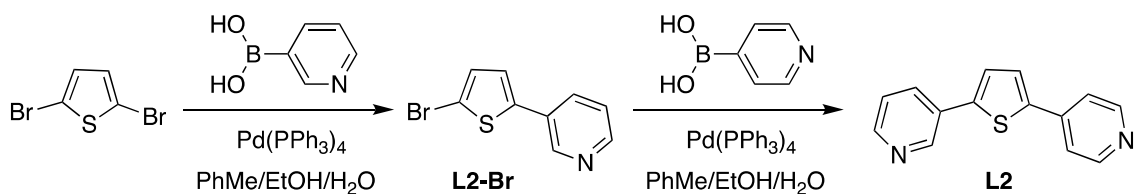


Figure S4. ¹³C NMR (101 MHz, CDCl₃) spectrum of ligand L1.



L2-Br : 2,5-Dibromothiophene (484 mg, 2.00 mmol), pyridin-3-ylboronic acid (123 mg, 1.00 mmol), Pd(PPh₃)₄ (115 mg, 995 μmol), and K₂CO₃ (0.6 g, 4.3 mmol) were combined in a 50 mL Schlenk tube. After vacuum/backfilling with N₂ for three times, 20 mL degassed toluene/EtOH/H₂O (2:1:1) was added with a syringe. The mixture was heated at 85 °C overnight. The reaction was cooled to RT, quenched with water, extracted with DCM (2 x 50 mL), washed with water (2 x 50 mL) and brine (50 mL), and dried over MgSO₄. The solvent was removed under reduced pressure, and the residue was purified by column chromatography on silica to yield **L2-Br** as a yellow powder (372 mg, 1.55 mmol, 77.5%). ¹H NMR (400 MHz, CDCl₃) δ 8.80 (d, *J* = 2.4 Hz, 1H), 8.54 (dd, *J* = 4.8, 1.5 Hz, 1H), 7.80 (ddd, *J* = 8.0, 2.4, 1.6 Hz, 1H), 7.34 (ddd, *J* = 8.0, 4.9, 0.9 Hz, 1H), 7.12 (d, *J* = 3.8 Hz, 1H), 7.08 (d, *J* = 3.9 Hz, 1H). ¹³C NMR (101 MHz, CDCl₃) δ 148.57, 146.43, 141.77, 133.20, 131.31, 130.02, 124.79, 124.01, 113.20. ESI-MS: *m/z* calculated for C₉H₆SNBr [M+H]⁺ 239.95, found 239.95.

L2 : Pyridin-4-ylboronic acid (185 mg, 1.51 mmol), **L2-Br** (300 mg, 1.25 mmol), Pd(PPh₃)₄ (81 mg, 70 μmol), and K₂CO₃ (0.6 g, 4.3 mmol) were combined in a 50 mL Schlenk tube. After vacuum/backfilling with N₂ for three times, 20 mL degassed toluene/EtOH/H₂O (2:1:1) was added with a syringe. The mixture was heated at 85 °C overnight. The reaction was cooled to RT, quenched with water, extracted with DCM (2 x 50 mL), washed with water (2 x 50 mL) and brine (50 mL), and dried over MgSO₄. The solvent was removed under reduced pressure, and the residue was purified by column chromatography on silica to yield **L2** as a yellow powder (241 mg, 1.01 mmol, 80.8%). ¹H NMR (400 MHz, CD₃CN) δ 8.93 (dd, *J* = 2.5, 0.9 Hz, 1H), 8.61 – 8.57 (m, 2H), 8.54 (dd, *J* = 4.8, 1.6 Hz, 1H), 8.02 (ddd, *J* = 8.0, 2.5, 1.6 Hz, 1H), 7.68 (d, *J* = 3.9 Hz, 1H), 7.62 – 7.57 (m, 2H), 7.55 (d, *J* = 3.9 Hz, 1H), 7.41 (ddd, *J* = 8.0, 4.8, 0.9 Hz, 1H). ¹³C NMR (101 MHz, CD₃CN) δ 151.49, 150.09, 147.56, 142.86, 142.10, 141.47, 133.75, 130.47, 128.14, 127.01, 124.85, 120.40. ESI-MS: *m/z* calculated for C₁₄H₁₁N₂S [M+H]⁺ 239.06, found 239.06.

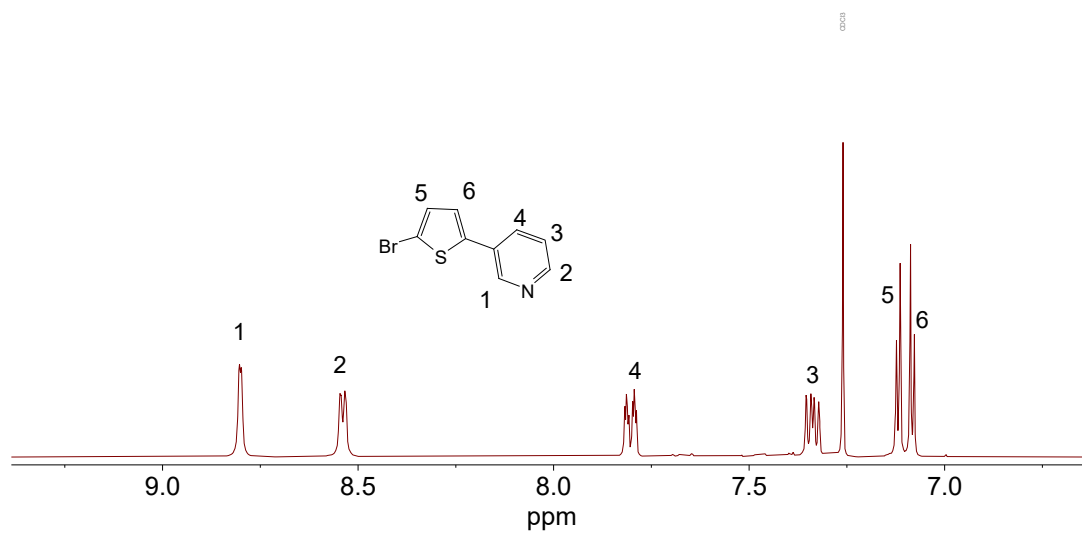


Figure S5. ¹H NMR (400 MHz, CDCl₃) spectrum of **L2-Br**.

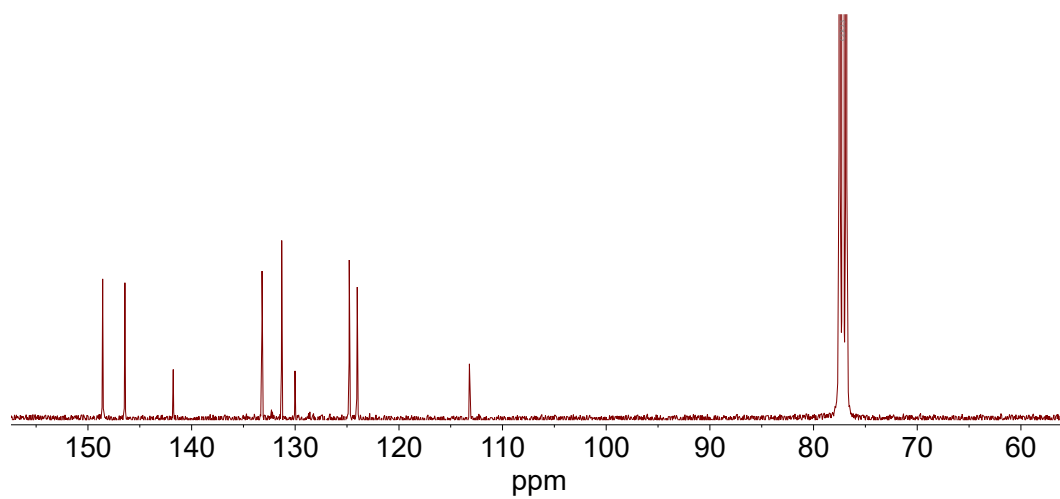


Figure S6. ¹³C NMR (101 MHz, CDCl₃) spectrum of **L2-Br**.

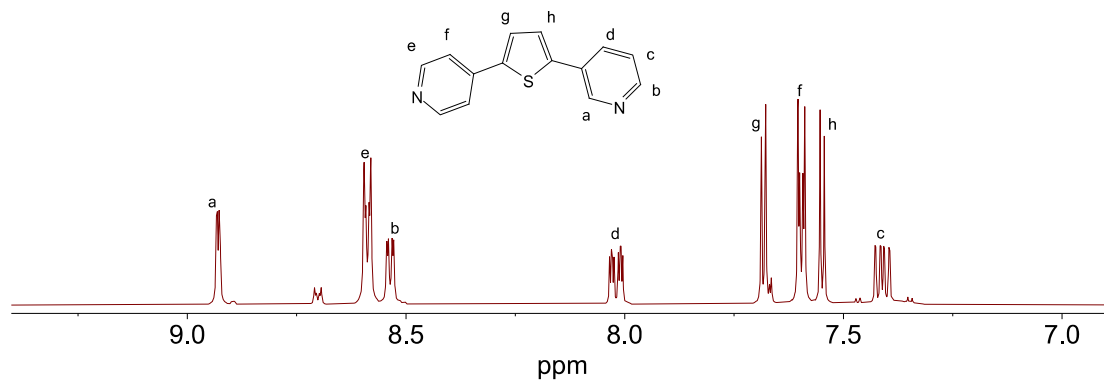


Figure S7. ¹H NMR (400 MHz, CD₃CN) spectrum of ligand L2.

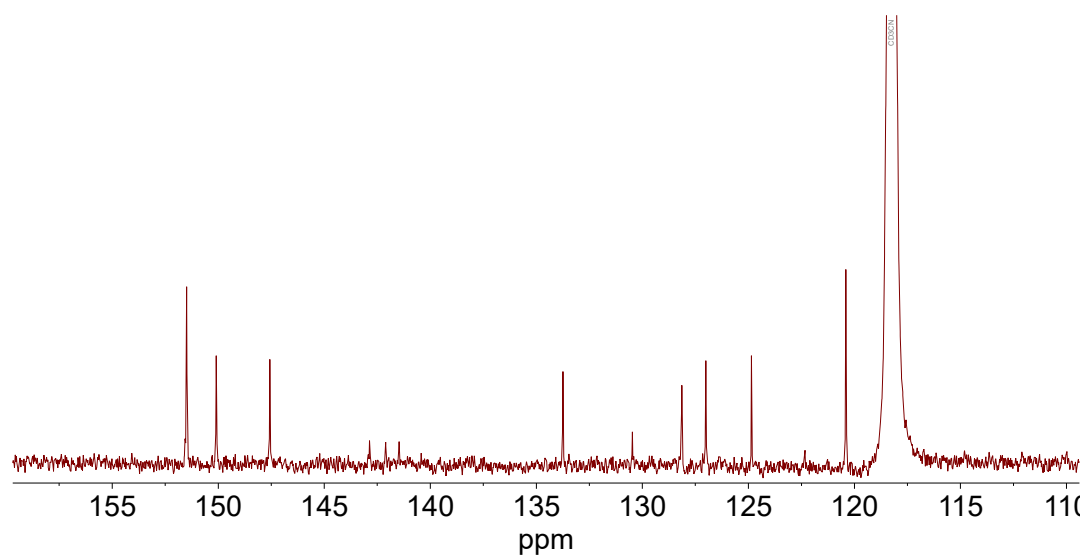
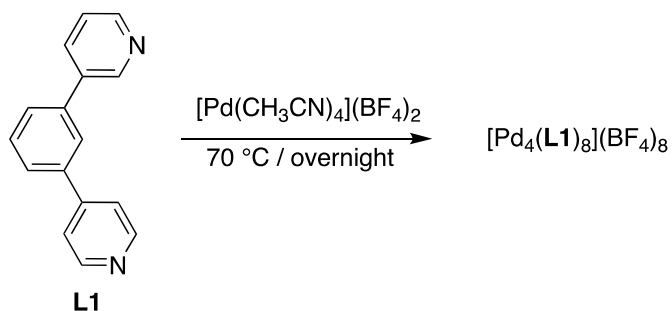


Figure S8. ¹³C NMR (101 MHz, CD₃CN) spectrum of ligand L2.

2.2 Syntheses of the cages



The cage compound $[\text{Pd}_4(\mathbf{L1})_8](\text{BF}_4)_8$ was synthesized by stirring a mixture of ligand **L1** (9 μmol , 200 μL of a 45 mM stock solution of **L1** in CD_3CN) and $[\text{Pd}(\text{CH}_3\text{CN})_4](\text{BF}_4)_2$ (4.5 μmol , 150 μL of a 30 mM stock solution in CD_3CN) in 650 μL CD_3CN at 70 $^\circ\text{C}$ overnight to give 1000 μL of a clear, colorless solution of cage $[\text{Pd}_4(\mathbf{L1})_8](\text{BF}_4)_8$ (1.125 mM). ^1H NMR (400 MHz, CD_3CN) δ 9.52 (d, $J = 2.0$ Hz, 4H), 9.48 (d, $J = 6.2$ Hz, 8H), 9.46 (d, $J = 1.5$ Hz, 8H), 9.38 (d, $J = 2.1$ Hz, 4H), 9.08 (dd, $J = 5.7, 1.3$ Hz, 4H), 8.81 (dd, $J = 5.7, 1.2$ Hz, 4H), 8.26 – 8.21 (m, 8H), 8.21 – 8.18 (m, 8H), 8.16 – 8.12 (m, 8H), 7.99 (d, $J = 2.0$ Hz, 4H), 7.85 (dt, $J = 6.6, 2.0$ Hz, 4H), 7.78 (dd, $J = 8.1, 5.6$ Hz, 4H), 7.75 – 7.71 (m, 4H), 7.69 (d, $J = 1.7$ Hz, 4H), 7.67 (t, $J = 7.7$ Hz, 4H), 7.64 – 7.61 (m, 4H), 7.61 – 7.58 (m, 4H), 7.57 (d, $J = 1.6$ Hz, 4H), 7.52 (t, $J = 7.7$ Hz, 4H). ^{13}C NMR (101 MHz, CD_3CN) δ 153.20, 152.58, 152.18, 151.22, 150.59, 149.48, 140.42, 139.56, 139.21, 137.83, 137.41, 137.03, 136.02, 131.61, 131.51, 131.06, 129.66, 129.37, 129.02, 128.47, 127.93, 127.68, 126.70, 126.07.

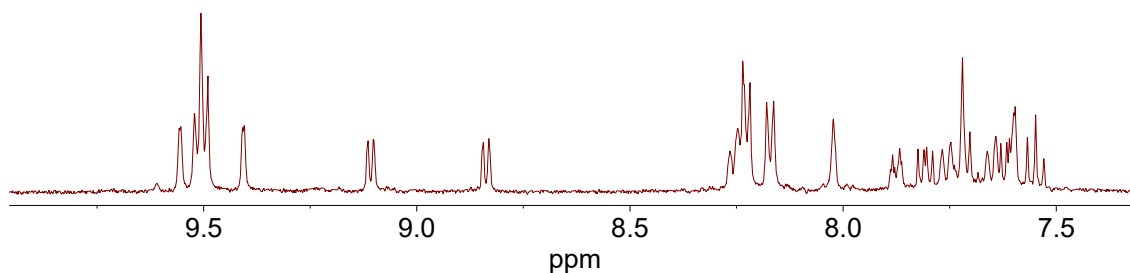


Figure S9. ^1H NMR spectra (400 MHz, CD_3CN) of $[\text{Pd}_4(\mathbf{L1})_8](\text{BF}_4)_8$.

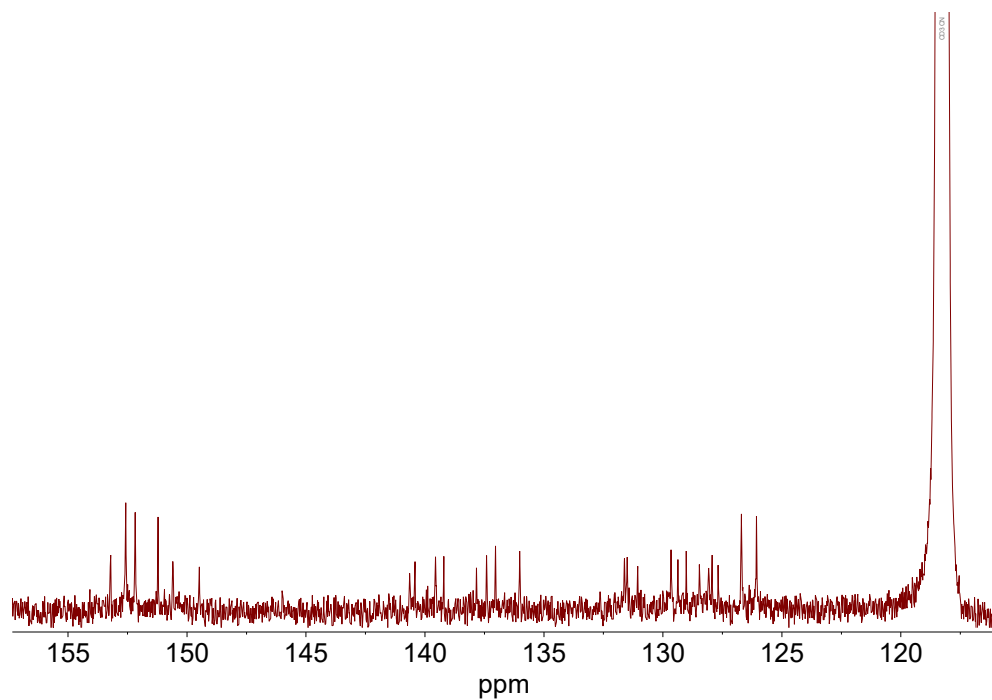


Figure S10. ^{13}C NMR spectra (101 MHz, CD_3CN) of $[\text{Pd}_4(\text{L1})_8](\text{BF}_4)_8$. The poor signal-to-noise ratio is a consequence of the low concentration of the cage.

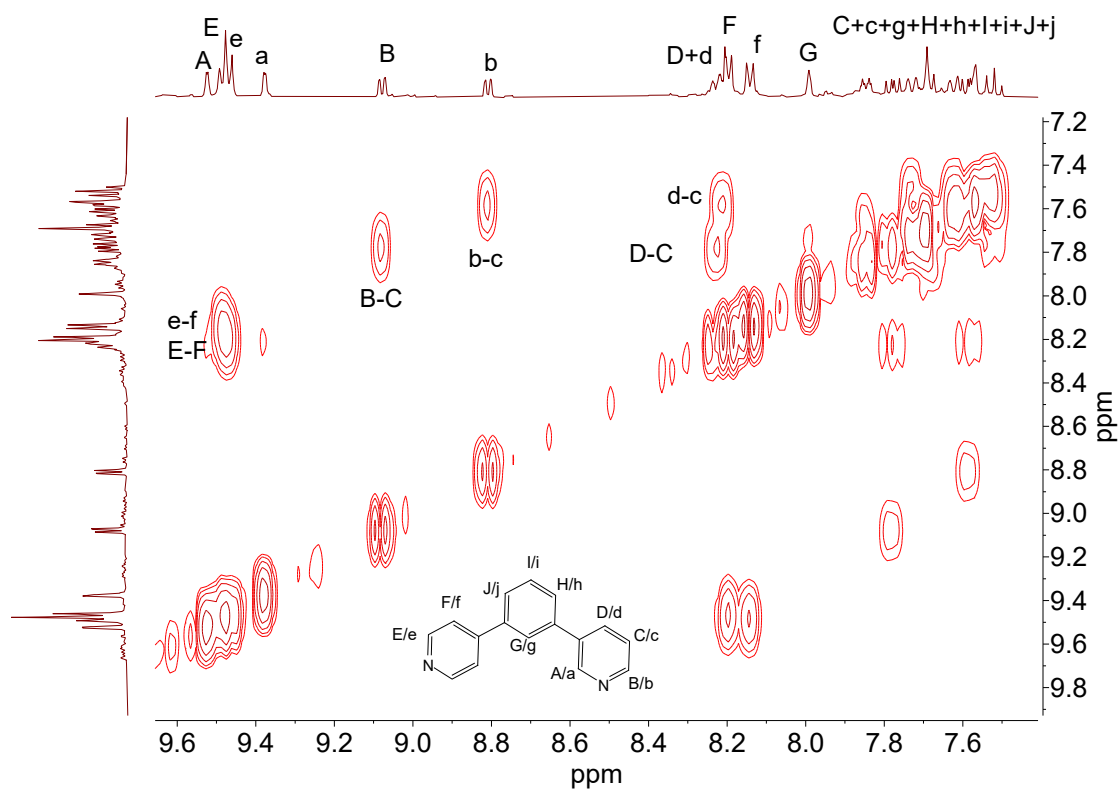


Figure S11. ^1H - ^1H COSY NMR spectrum (400 MHz, CD_3CN) of $[\text{Pd}_4(\text{L1})_8](\text{BF}_4)_8$.

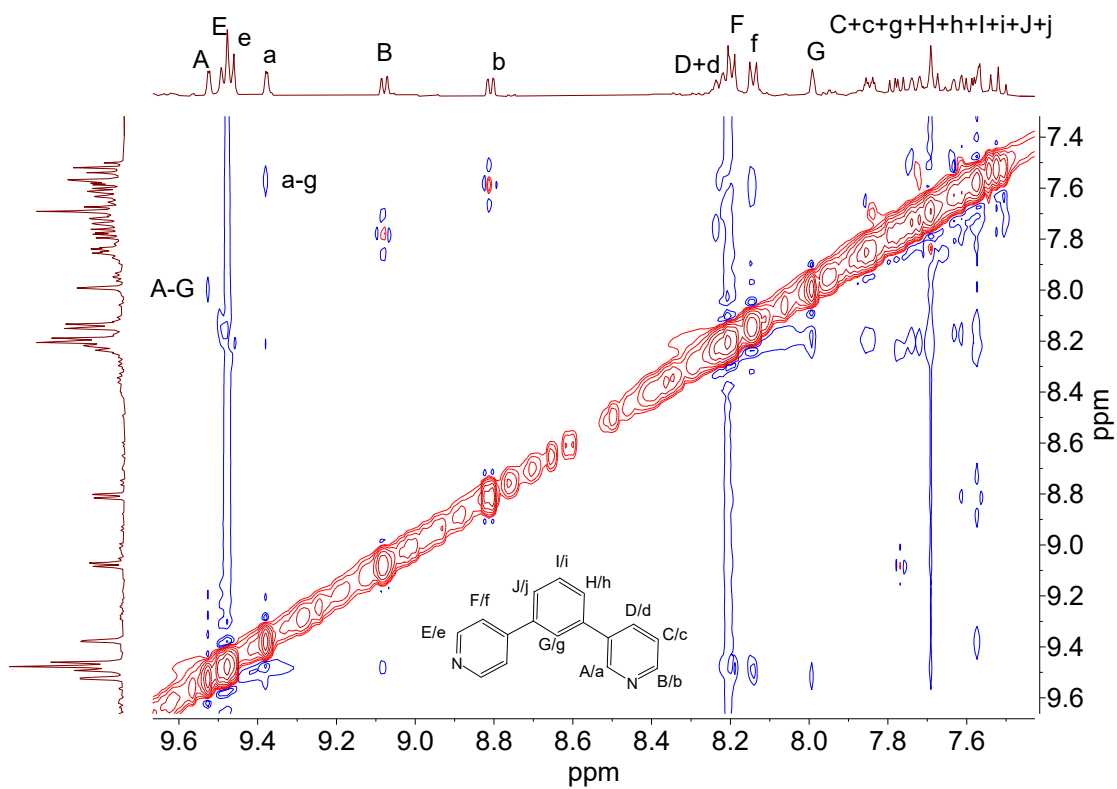


Figure S12. ^1H - ^1H NOESY NMR spectrum (400 MHz, CD_3CN) of $[\text{Pd}_4(\text{L1})_8](\text{BF}_4)_8$.

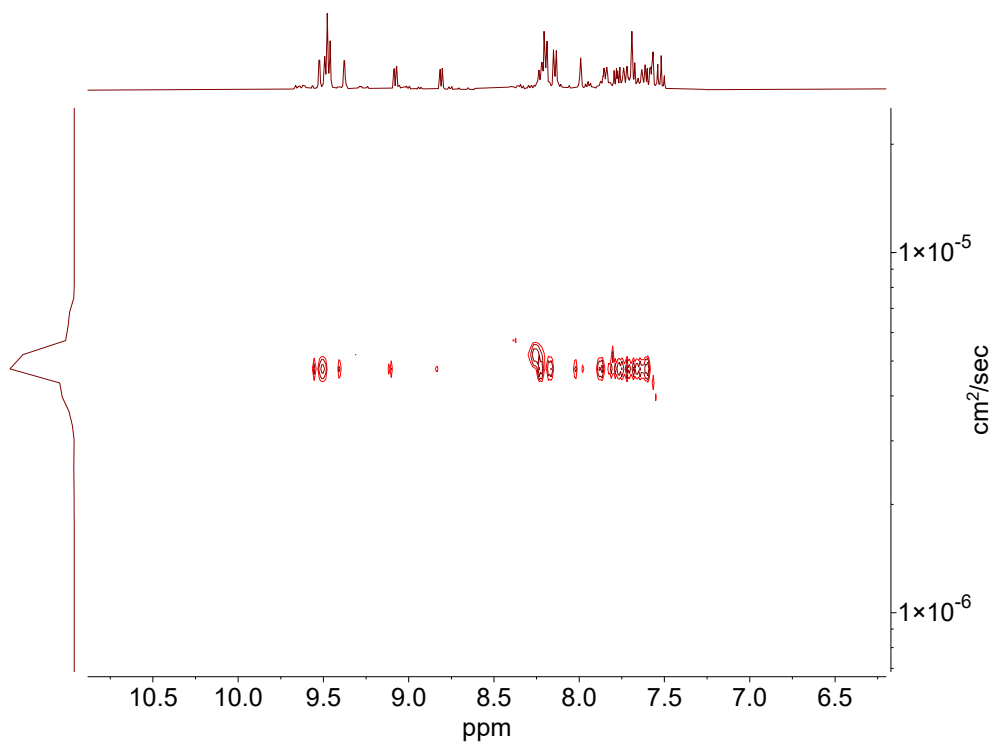


Figure S13. ^1H - ^1H DOSY NMR spectrum (400 MHz, CD_3CN) of $[\text{Pd}_4(\text{L1})_8](\text{BF}_4)_8$.

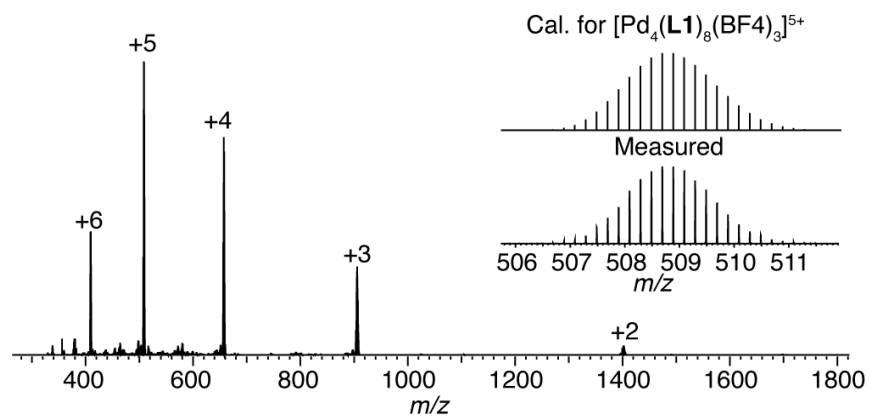
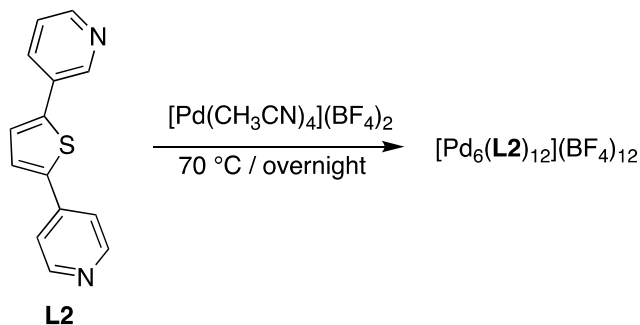


Figure S14. High-resolution ESI mass spectrum of $[\text{Pd}_4(\text{L1})_8(\text{BF}_4)_x]^{8-x}$ ($x = 2-6$).



The cage compound $[\text{Pd}_6(\mathbf{L2})_{12}](\text{BF}_4)_{12}$ was synthesized in quantitative yield by stirring a mixture of ligand **L2** (9 μmol , 200 μL of a 45 mM stock solution of **L2** in CD_3CN) and $[\text{Pd}(\text{CH}_3\text{CN})_4](\text{BF}_4)_2$ (4.5 μmol , 150 μL of a 30 mM stock solution in CD_3CN) in 650 μL CD_3CN at 70 $^\circ\text{C}$ overnight to give 1000 μL of a pale yellow, slightly turbid solution of cage $[\text{Pd}_6(\mathbf{L2})_{12}](\text{BF}_4)_{12}$ (0.75 mM). ^1H NMR (400 MHz, CD_3CN) δ 9.50 (d, $J = 2.0$ Hz, 6H), 9.47 (d, $J = 2.1$ Hz, 6H), 9.23 (dd, $J = 5.8, 1.2$ Hz, 6H), 9.19 (d, $J = 1.2$ Hz, 6H), 9.18 (s, 12H), 9.16 – 9.12 (m, 12H), 8.29 (dddd, $J = 11.6, 8.3, 2.2, 1.2$ Hz, 12H), 7.90 – 7.79 (m, 24H), 7.77 – 7.67 (m, 24H), 7.59 (d, $J = 4.1$ Hz, 6H), 7.55 (d, $J = 4.1$ Hz, 6H). ^{13}C NMR (101 MHz, CD_3CN) δ 152.07, 152.00, 150.75, 150.67, 149.09, 148.91, 145.40, 145.34, 142.10, 142.07, 140.79, 140.76, 137.87, 137.36, 133.73, 133.63, 131.24, 131.08, 129.89, 129.72, 128.69, 128.64, 123.62, 123.45.

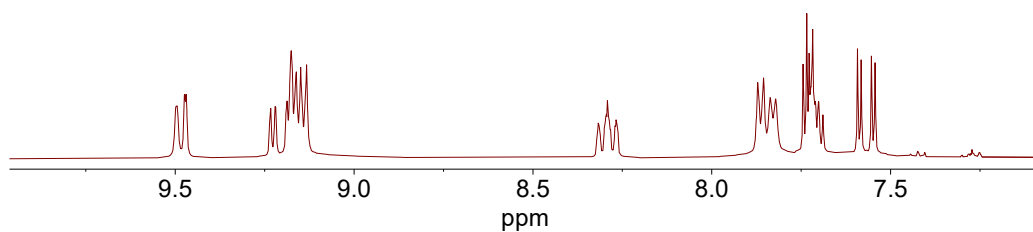


Figure S15. ^1H NMR spectra (400 MHz, CD_3CN) of $[\text{Pd}_6(\mathbf{L2})_{12}](\text{BF}_4)_{12}$.

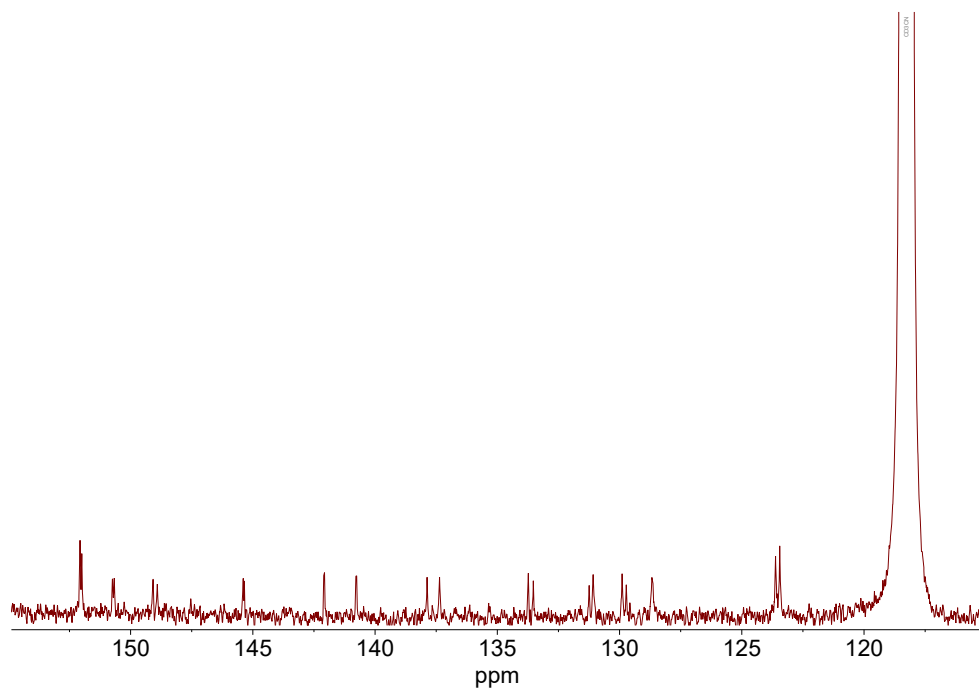


Figure S16. ^{13}C NMR spectra (101 MHz, CD_3CN) of $[\text{Pd}_6(\text{L}2)_{12}](\text{BF}_4)_{12}$. The poor signal-to-noise ratio is a consequence of the low concentration of the cage.

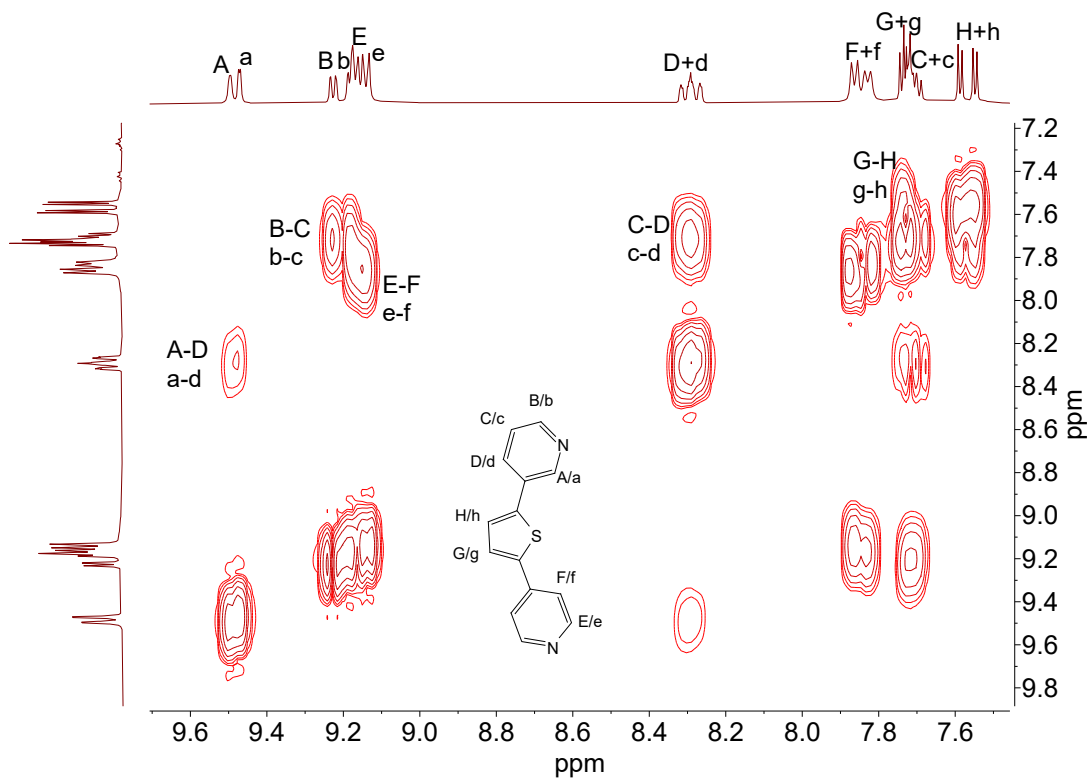


Figure S17. ^1H - ^1H COSY NMR spectrum (400 MHz, CD_3CN) of $[\text{Pd}_6(\text{L}2)_{12}](\text{BF}_4)_{12}$.

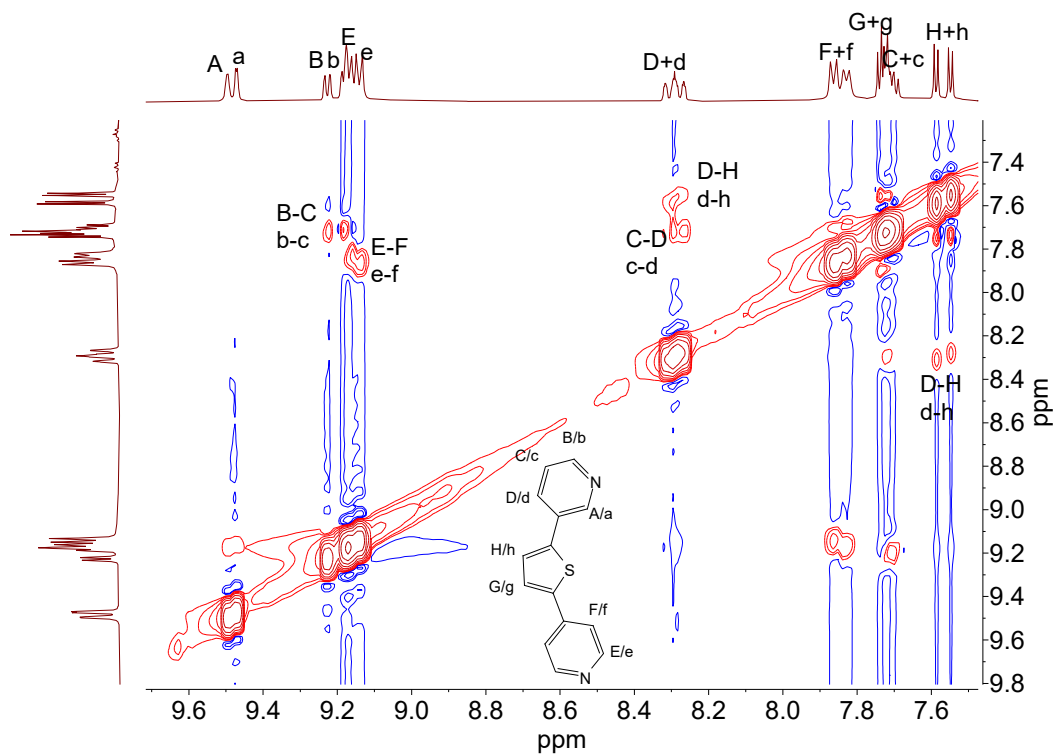


Figure S18. ^1H - ^1H NOESY NMR spectrum (400 MHz, CD_3CN) of $[\text{Pd}_6(\text{L}2)_{12}](\text{BF}_4)_{12}$.

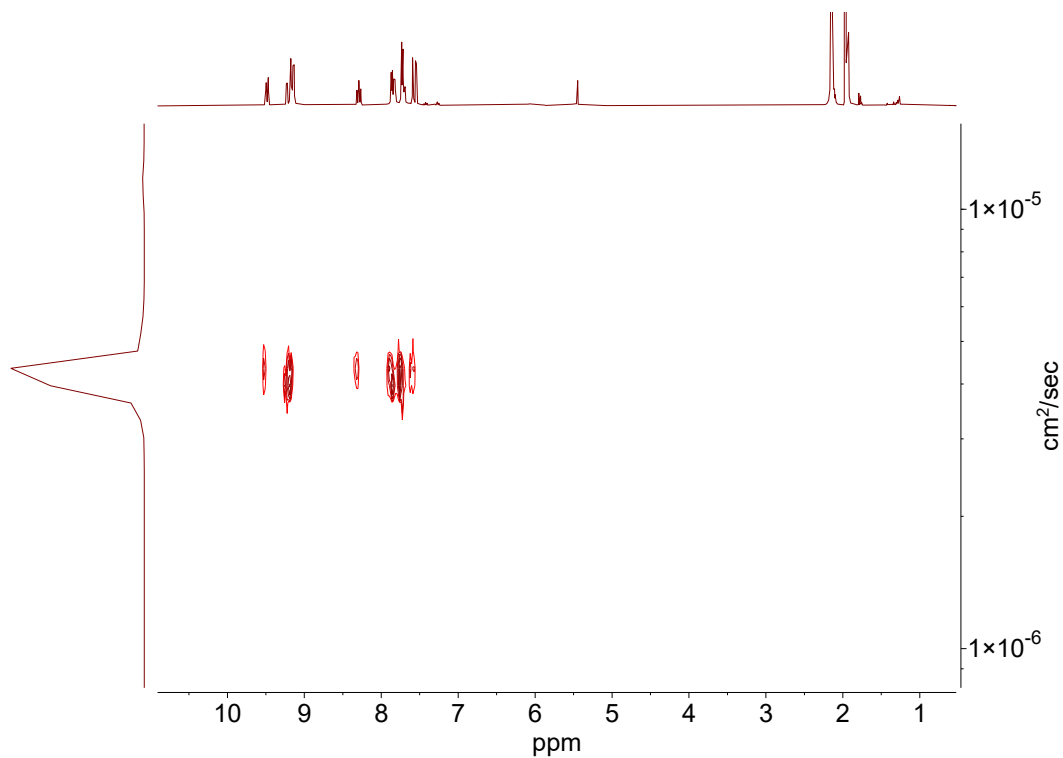


Figure S19. ^1H - ^1H DOSY NMR spectrum (400 MHz, CD_3CN) of $[\text{Pd}_6(\text{L}2)_{12}](\text{BF}_4)_{12}$.

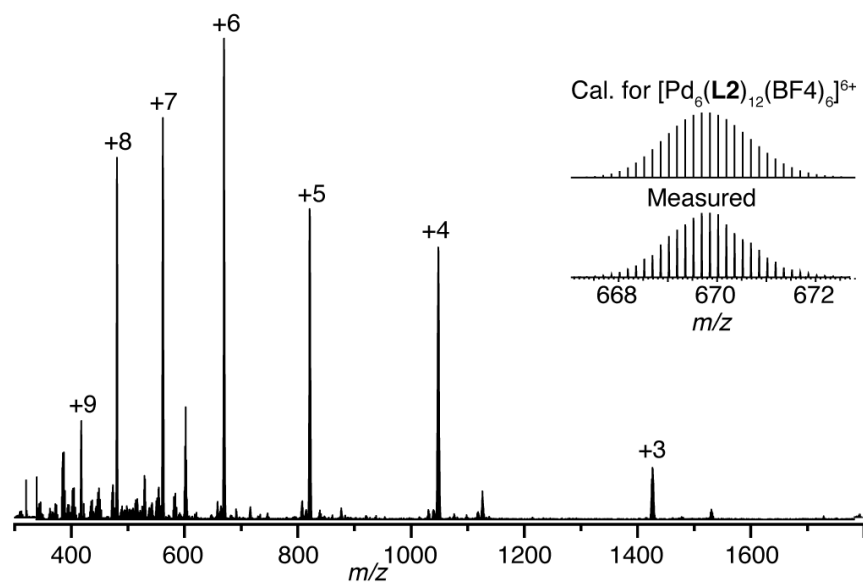


Figure S20. High-resolution ESI mass spectrum of $[\text{Pd}_6(\text{L2})_{12}(\text{BF}_4)_x]^{12-x}$ ($x = 3-9$).

3 Titration

Host-guest titrations were performed at RT by stepwise addition of a stock solution of NaBPh₄ (CD₃CN, 90 mM) to 500 μ L of a solution of [Pd₄(L1)₈](BF₄)₈ (1.125 mM) in CD₃CN in an NMR tube. The ¹H NMR spectra were recoded immediately after briefly shaking the solution. Association constants were calculated using Thordarson's online tool Bindfit (<http://app.supramolecular.org/bindfit/>).

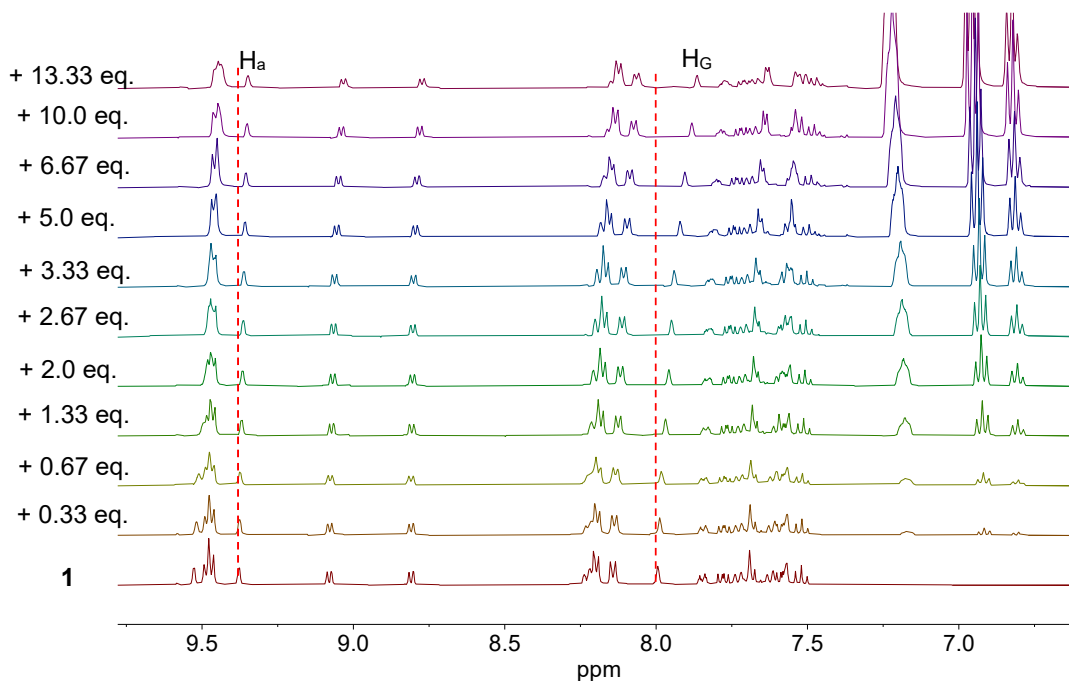


Figure S21. ¹H NMR spectra (400 MHz, CD₃CN) of a solution of cage [Pd₄(L1)₈](BF₄)₈ with increasing amounts of NaBPh₄.

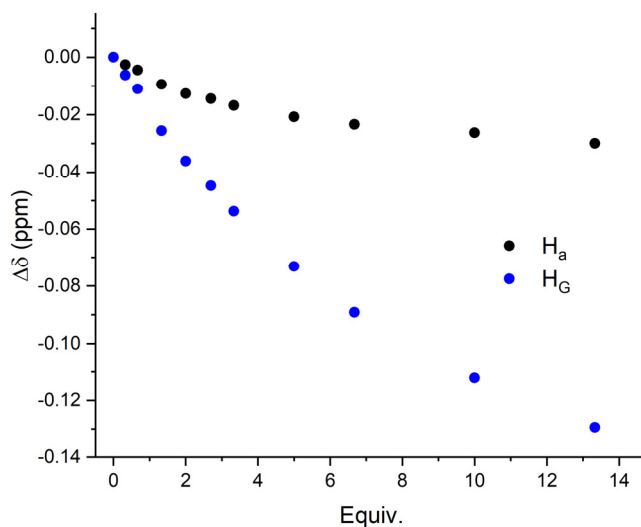


Figure S22. Complexation-induced shift of the signals of H_a and H_G. Fitting the data to a 1 : 1 binding model resulted in an association constant of $K_a = 82 \text{ M}^{-1}$.

4 Control experiments

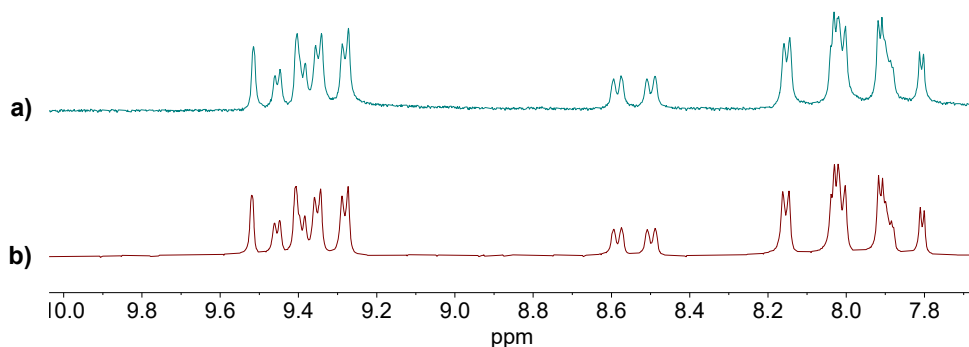
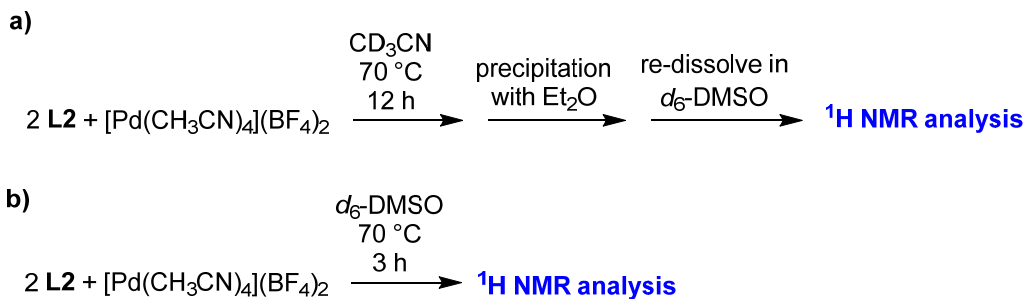


Figure S23. ^1H NMR spectra (400 MHz, d_6 -DMSO) of $[\text{Pd}_6(\text{L2})_{12}](\text{BF}_4)_{12}$. **a)** The sample was prepared as described above in acetonitrile. The product was precipitated with excess diethyl ether, collected by centrifugation, dried under high vacuum, and then re-dissolved in d_6 -DMSO. Subsequently, a ^1H NMR spectrum was recorded. **b)** The sample was prepared *in situ* in d_6 -DMSO, and a ^1H NMR spectrum was recorded.

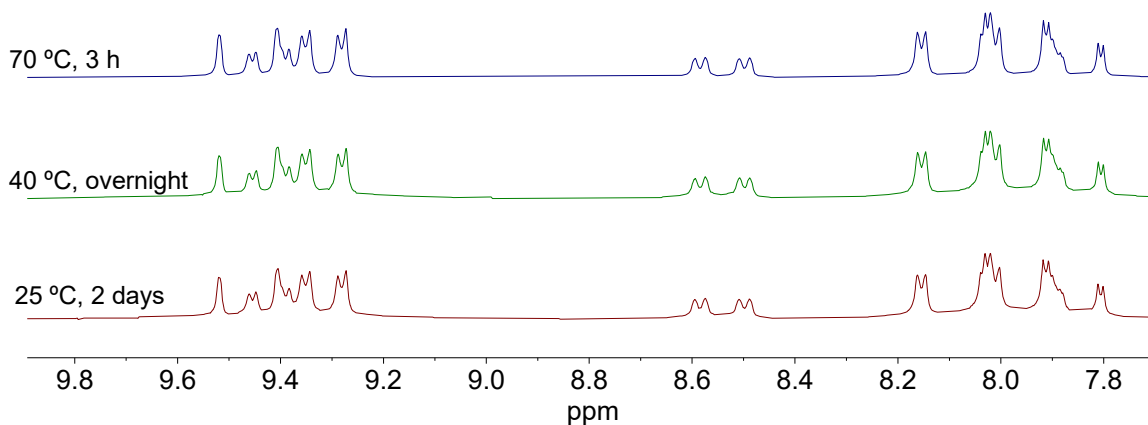


Figure S24. ^1H NMR spectra (400 MHz, d_6 -DMSO, 298 K) of $[\text{Pd}_6(\text{L2})_{12}](\text{BF}_4)_{12}$. The samples were all prepared *in situ* in d_6 -DMSO at the same concentration ($[\text{L2}] = 9 \text{ mM}$), but at different temperatures and with different reaction times: 70 °C for 3 h (top); 40 °C overnight (middle), and room temperature for 2 days (bottom).

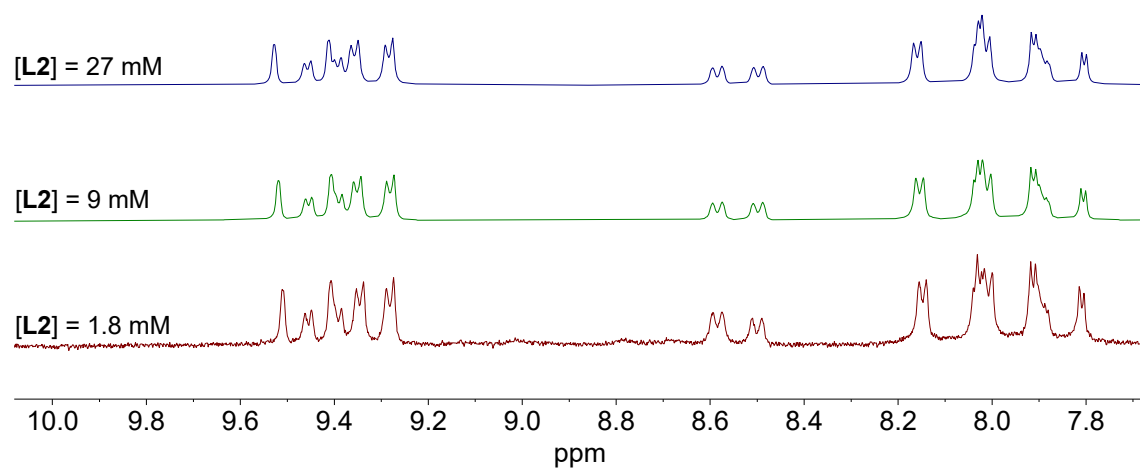


Figure S25. ¹H NMR spectra (400 MHz, d₆-DMSO, 298 K) of [Pd₆(L₂)₁₂](BF₄)₁₂. The samples were all prepared at 70 °C for 3 h but with different concentrations: [L₂] = 27 mM (top); [L₂] = 9 mM (middle) and [L₂] = 1.8 mM (bottom).

5 Analysis of potential isomers

Our approach for enumerating possible isomers uses the standard “orbit-stabilizer” method.¹ Each n -ligand isomer is assigned a vector in $\{-1, 1\}^n$ depending on the orientation of each of the ligands. All of the symmetries of interest (rotations and reflections) act on this set of vectors via multiplication by signed permutation matrices. In each case, the rotational symmetry group can be generated by two rigid motions (with a third generator provided by a single reflection when we wish to find chiral symmetries). This allows us to delegate the group construction, orbit computations, and comparisons to a computer in a straightforward way.

4.1 Translation into vectors and matrices

We first explain our method for translating the orientations of n ligands into a vector $v \in \{-1, 1\}^n$. We fix an initial configuration of metals and ligand sites (places where ligands will go). The formation of an isomer will result in each ligand site receiving a ligand in one of two orientations. For clarity, we will call an assignment of orientations to each of the ligand sites an ordering. We then give labels

- M_1, \dots, M_m to each of the m metals, and
- L_1, \dots, L_n to each of the n ligand sites.

Let L_i be a ligand site connecting two metals M_j and M_k . Given an ordering x , we will say that L_i has positive orientation in x if the ligand at that site begins at $M_{\min\{j,k\}}$ and ends at $M_{\max\{j,k\}}$. Otherwise, we will say it has negative orientation. This gives a natural translation of each possible ordering to a vector v with

$$v_j = \begin{cases} +1 & \text{if } L_j \text{ has positive orientation} \\ -1 & \text{if } L_j \text{ has negative orientation} \end{cases}$$

As mentioned above, all of the symmetries of interest (both rotations and reflections) correspond to signed permutation matrices in a natural way. Each symmetry results in a permutation π of the metals $M_i \rightarrow M_{\pi(i)}$ as well as a permutation δ of the ligand sites $L_i \rightarrow L_{\delta(i)}$. For each ligand site L_i with connecting metals M_j and M_k with $j < k$, the associated matrix will have entry

$$A_{i,\sigma(i)} = \begin{cases} +1 & \text{if } \pi(j) < \pi(k) \\ -1 & \text{if } \pi(j) > \pi(k) \end{cases}$$

and $A_{i,t} = 0$ for all other t .

4.2 Integer labels

For the purpose of presentation, we will assign each ordering x_i a unique integer N_i with $0 \leq N_i \leq 2^n - 1$. In particular, if $v^i \in \{-1, 1\}^n$ is the vector of ligand orientations mentioned above, we can transform between v^i and N_i in a standard way using the (unique) binary representation of each N_i as follows:

$$N_i = \sum_{j=1}^n 2^{(v_{n-j+1}^i + 1)/2}.$$

In reverse, if $b_{n-1} \dots b_1 b_0$ is the binary representation of N_i with each $b_j \in \{0, 1\}$ (and with extra 0's added on the left if necessary), then we can recover the vector v^i using the formula

$$v_j^i = 2b_{n-j} - 1.$$

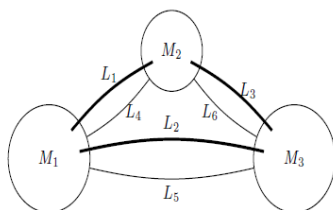
For example, in the case where $n = 6$ and $N_i = 13$, we have that the binary representation of 13 is 1101, which we pad on the left with 0's to make it have 6 digits: 001101 and then form the vector $(-1, -1, +1, +1, -1, +1)$. Similarly, in the case where $n = 8$ and $N_i = 16$, we have that the binary representation of 16 is 10000, which we pad on the left with 0's to make it have 8 digits: 00010000 and then form the vector $(-1, -1, -1, +1, -1, -1, -1, -1)$.

4.3 Results

In each of the sections below, we provide a list of the unique (under rotational symmetries) isomers for the configurations M_3L_6 , M_4L_8 , and M_6L_{12} using the integer labels discussed in the previous section. In particular, we give a diagram showing the labels of metals and ligand sites that were used to generate the vectors and matrices and then describe the rotational symmetry group as it acts on the diagram. The isomers are sorted according to the number of different orderings that are considered "equivalent" to the given representative. Chiral pairs are grouped together in brackets. All computations were done in Mathematica using code that is publicly available at: <https://doi.org/10.5281/zenodo.5090646>

M_3L_6

All permutations of the metals are possible to achieve via rotations, forming the rotation group D_3 . The dark lines in the diagram show the subgroup generated by the planar rotation $M_1 \rightarrow M_2 \rightarrow M_3 \rightarrow M_1$.



12 orderings each: 0, {2, 13}, {3, 6}, {5, 10}

6 orderings each: {1, 8}, {4, 11}, {7, 14}

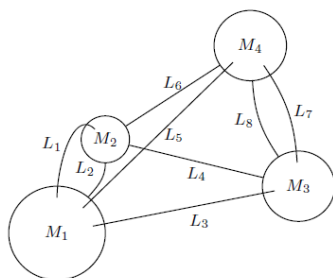
4 orderings each: 18

2 orderings each: {21, 42}

M₄L₈

The asymmetry in the double ligands restricts each isomer to having at most 4 valid rotational symmetries, forcing the symmetry group to be either $S_2 \times S_2$ or C_4 . It is easy to see that it must be the former by noticing that

1. the 180° rotation around the line through the midpoints of L_3 and L_6 (which takes L_1 to L_8)
 2. the 180° rotation around the line through the midpoints of L_4 and L_5 (which takes L_1 to L_7)
- are distinct elements of degree 2 (which can only exist $S_2 \times S_2$).

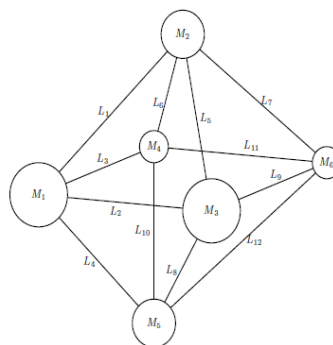


4 orderings each: {0, 3}, {1, 2}, {4, 11}, {5, 10}, {6, 9}, {7, 8}, {12, 15}, {13, 14}, {16, 35}, {17, 34}, {18, 33}, {19, 28}, {20, 43}, {21, 42}, {22, 41}, {24, 27}, {25, 38}, {26, 37}, {29, 46}, {30, 45}, {49, 50}, {53, 58}, {54, 57}, {61, 62}, {69, 109}, {70, 137}, {73, 93}, {74, 133}, {77, 85}, {78, 141}

2 orderings each: 89, 101, {65, 125}, {66, 129}, {90, 153}

M₆L₁₂

The rotational symmetries are the same as those of a cube (the labels used in the diagram map metal M_i to the face of a standard 6-sided die with i pips). This can be seen to be isomorphic to S_4 (acting transitively on the 4 diagonals of the cube).



24 orderings each: 0, 1, 6, 7, 8, 9, 14, 31, 49, 50, 55, 59, 64, 65, 70, 71, 72, 73, 94, 206, 215, 222, 238, 301, 313, {2, 4}, {3, 5}, {10, 12}, {11, 13}, {16, 32}, {17, 33}, {18, 36}, {19, 37}, {20, 34}, {21, 35}, {22, 38}, {23, 39}, {24, 40}, {25, 41}, {26, 44}, {27, 45}, {28, 42}, {29, 43}, {30, 46}, {51, 53}, {66, 68}, {67, 69}, {74, 76}, {75, 77}, {80, 96}, {81, 97}, {82, 100}, {83, 101}, {84, 98}, {85, 99}, {86, 102}, {87, 103}, {88, 104}, {89, 105}, {90, 108}, {91, 109}, {92, 106}, {93, 107}, {145, 453}, {147, 449}, {151, 223}, {192, 365}, {193, 220}, {194, 361}, {195, 450}, {196, 433}, {197, 212}, {198, 582}, {199, 443}, {200, 333}, {202, 329}, {204, 462}, {208, 229}, {209, 323}, {210, 291}, {211, 355}, {213, 339}, {214, 307}, {216, 225}, {217, 322}, {218, 290}, {219, 221}, {224, 436}, {227, 458}, {228, 432}, {230, 316}, {297, 312}, {298, 435}

12 orderings each: 15, 48, 54, 57, 78, 315, 317, 330, {150, 550}, {231, 599}

8 orderings each: 467, {232, 600}, {289, 440}, {345, 838}

6 orderings each: 63, 119, 159, {144, 485}

2 orderings: 1337

6 Crystallographic analyses

Single light yellow-grey block crystal of $[\text{Pd}_4(\mathbf{L1})_8][\text{Na}(\text{BF}_4)_4](\text{BPh}_4)_2(\text{BF}_4)_3$ were obtained by slow vapor diffusion of THF/Et₂O (v/v = 1 : 1) into a acetonitrile solution of $[\text{Pd}_4(\mathbf{L1})_8](\text{BF}_4)_8$ (1.125 mM) with 5.0 equiv. of NaBPh₄. Single crystal of $[\text{Pd}_6(\mathbf{L2})_{12}](\text{BPh}_4)_8$ (some anions could not be refined) were obtained by adding an excess (20.0 equiv) NaBPh₄ into a acetonitrile solution of $[\text{Pd}_6(\mathbf{L2})_{12}](\text{BF}_4)_{12}$ (0.75 mM) overnight.

Bragg-intensities of $[\text{Pd}_4(\mathbf{L1})_8][\text{Na}(\text{BF}_4)_4](\text{BPh}_4)_2(\text{BF}_4)_3$ and $[\text{Pd}_6(\mathbf{L2})_{12}](\text{BPh}_4)_4(\text{X})_8$ were collected at low temperature using CuK α radiation. A Rigaku SuperNova dual system diffractometer with an AtlasS2 CCD detector was used. The datasets were reduced and corrected for absorption, with the help of a set of faces enclosing the crystals as snugly as possible, with the latest available version of *CrysAlisPro*.² The solutions and refinements of the structures were performed by the latest available version of *ShelXT*³ and *ShelXL*⁴ using *Olex2*⁵ as the graphical interface. All non-hydrogen atoms were refined anisotropically using full-matrix least-squares based on $|F|^2$. The hydrogen atoms were placed at calculated positions by means of the “riding” model where each H-atom was assigned a fixed isotropic displacement parameter with a value equal to 1.2 U_{eq} of its parent C-atom (1.5 U_{eq} for the methyl groups). The RIGU and SIMU restraints were applied to the displacement parameters of all non-hydrogen atoms. Additional counter-ions and solvent molecules, too disordered to be located in the electron density map, were taken into account using the *Olex2* solvent-mask procedure.⁵

In the structure $[\text{Pd}_4(\mathbf{L1})_8][\text{Na}(\text{BF}_4)_4](\text{BPh}_4)_2(\text{BF}_4)_3$, a solvent mask was calculated and 2272 electrons were found in a volume of 11740 Å³. This is consistent with the presence of three and a half THF-solvent molecules per asymmetric unit, namely three in a void of 650, half in a void of 68 and none in a void of 16, which accounts for 2240 electrons per unit cell. It should be noticed that the diethyl ether recrystallisation solvent could not be unambiguously identified in a difference map. Possibly, it appeared as a superposition of very disordered THF solvent molecules, but this assignment was way too fragile and uncertain to include diethyl ether in the calculation of the solvent-masking program in *Olex2* (knowing the number of the electrons in THF and diethyl ether to be very close; 40 vs. 42 electrons).

In the structure $[\text{Pd}_6(\mathbf{L2})_{12}](\text{BPh}_4)_8$, a solvent mask was calculated and 1118 electrons were found in a volume of 4466 Å³ in one void per unit cell. This is consistent with the presence of two BPh₄⁻ counter-ions and ten acetonitrile-solvent molecules per asymmetric unit, which accounts for 558 electrons per unit cell.

Crystallographic and refinement data are summarized in **Table S1** for $[\text{Pd}_4(\mathbf{L1})_8][\text{Na}(\text{BF}_4)_4](\text{BPh}_4)_2(\text{BF}_4)_3$ and $[\text{Pd}_6(\mathbf{L2})_{12}](\text{BPh}_4)_8$. Crystallographic data have been deposited with the Cambridge Crystallographic Data Centre and correspond to the following codes: $[\text{Pd}_4(\mathbf{L1})_8][\text{Na}(\text{BF}_4)_4](\text{BPh}_4)_2(\text{BF}_4)_3$ (2093068), $[\text{Pd}_6(\mathbf{L2})_{12}](\text{BPh}_4)_8$ (2092340). These data can be obtained free of charge via www.ccdc.cam.ac.uk/data_request/cif.

Table S1. Crystal data and structure refinement for [Pd₄(L1)₈][Na(BF₄)₄](BPh₄)₂(BF₄)₃ and [Pd₆(L2)₁₂](BPh₄)₈

Compound	[Pd ₄ (L1) ₈][Na(BF ₄) ₄](BPh ₄) ₂ (BF ₄) ₃	[Pd ₆ (L2) ₁₂](BPh ₄) ₈
Formula	C ₁₇₆ H ₁₃₆ B ₉ F ₂₈ N ₁₆ NaPd ₄	C ₃₆₀ H ₂₇₈ B ₈ N ₂₄ Pd ₆ S ₁₂
<i>D</i> _{calc.} / g cm ⁻³	1.171	0.939
μ /mm ⁻¹	3.474	2.877
Formula Weight	3552.88	6049.65
Colour	clear pale yellow	clear light yellow
Shape	prism-shaped	plate-shaped
Size/mm ³	0.39×0.35×0.30	0.24×0.17×0.05
<i>T</i> /K	140.00(10)	140.00(10)
Crystal System	orthorhombic	triclinic
Space Group	<i>Cc</i>	<i>P</i> $\bar{1}$
<i>a</i> /Å	30.1520(5)	22.4855(10)
<i>b</i> /Å	39.3021(10)	22.5246(9)
<i>c</i> /Å	33.9980(6)	25.9711(13)
α /°	90	65.278(5)
β /°	90	69.004(4)
γ /°	90	67.104(4)
<i>V</i> /Å ³	40288.9(14)	10702.0(10)
<i>Z</i>	8	1
<i>Z'</i>	0.5	0.5
Wavelength/Å	1.54184	1.54184
Radiation type	CuK α	CuK α
θ _{min} /°	3.189	3.241
θ _{max} /°	72.696	50.721
Measured Refl's.	97504	57926
Ind't Refl's	19734	21834
Refl's with <i>I</i> > 2 σ (<i>I</i>)	13293	13360
<i>R</i> _{int}	0.0461	0.1222
Parameters	1133	1516
Restraints	1847	2993
Largest Peak/e Å ⁻³	2.185	3.003
Deepest Hole/e Å ⁻³	-1.405	-2.081
GooF	1.032	1.899
<i>wR</i> ₂ (all data)	0.3227	0.5476
<i>wR</i> ₂	0.2831	0.5045
<i>R</i> ₁ (all data)	0.1280	0.2797
<i>R</i> ₁	0.0985	0.2192
CCDC number	2093068	2092340

7 References

- [1] D. S. Dummit and R. M. Foote, *Abstract Algebra, 3rd Ed.*, Wiley-VCH, 2003.
- [2] *CrysAlis^{Pro}* software system, Rigaku Oxford Diffraction, (2021).
- [3] G. M. Sheldrick, *Acta Cryst.*, 2015, **A71**, 3–8.
- [4] G. M. Sheldrick, *Acta Cryst.*, 2015, **C71**, 3–8.
- [5] O. V. Dolomanov, J. L. Bourhis, R. J. Gildea, J. A. K. Howard and H. Puschmann, *J. Appl. Cryst.*, 2009, **42**, 339–341.